CrystEngComm

PAPER

View Article Online
View Journal | View Issue

Cite this: *CrystEngComm*, 2019, **21**, 1772

Ferrocenecarboxylic acid: a functional modulator for UiO-66 synthesis and incorporation of Pd nanoparticles†

Zheng Deng,[ab] Xinsheng Peng *[b] and Yu-Jia Zeng *[a]

Received 14th January 2019,
Accepted 29th January 2019

DOI: 10.1039/c9ce00067d

rsc.li/crystengcomm

Modulators were frequently employed to synthesize UiO-66 with improved crystallinity, enhanced porosity, and controlled size and morphology. However, little attention was paid to the functionality of modulators themselves. We showed that ferrocenecarboxylic acid (FcCOOH) was not only an efficient modulator for UiO-66 synthesis but also endowed UiO-66 with redox properties. FcCOOH significantly reduced the size of UiO-66 from 400 nm intergrown crystals into 50 nm individual ones, and at the same time remarkably improved their crystallinity, micro-pore volume (0.56 $cm^3\ g^{-1}$), and BET surface area (1364 $m^2\ g^{-1}$). In addition, FcCOOH in UiO-66 served as a reducing agent for *in situ* incorporation of Pd nanoparticles into UiO-66 under mild conditions and was used as an efficient heterogeneous catalyst for the Suzuki–Miyaura reaction.

1. Introduction

Metal–organic frameworks (MOFs) are well-known as fascinating porous materials and found to have tremendous applications in catalysis,[1,2] electrochemisty,[3] gas storage[4,5] and separation,[6,7] *etc.* Among the hundreds of MOFs synthesized to date, Zr-based MOFs have attracted considerable interest due to their exceptional thermal, chemical and mechanical stabilities[8] which originated from the high affinity of zirconium towards oxygen and their high degree of connectivity.[9]

UiO-66 is the prototype of Zr-based MOFs. It has a face-centred-cubic crystal structure and each $Zr_6O_4(OH)_4$ cluster is connected to 12 terephthalic acid (H_2BDC) molecules to form a 3D framework.[8] The crystallinity, morphology and internal structure of UiO-66 crystals can be modulated by adding a sufficient amount of monocarboxylic acid (*e.g.* formic acid,[10] acetic acid, benzoic acid,[11] *etc.*) during synthesis. Furthermore, modulators also enhance the reproducibility of the synthesis procedure.[12] It is believed that modulators affect the coordination equilibrium between $Zr_6O_4(OH)_4$ clusters and H_2BDC through competing with H_2BDC for coordination sites.[11] Thus, the nucleation and growth rates of UiO-66 crystals are changed, leading to the formation of crystals with a higher degree of crystallinity and controlled morphology and size. Behrens and co-workers[11] were one of the pioneering groups who used monocarboxylic acid to modulate the synthesis of Zr-based MOFs and found that UiO-66 crystals could be modulated by varying the amount of the modulator (benzoic or acetic acid). Once the concentration of the modulator increased, the obtained UiO-66 changed from intergrown crystals into individual ones, and their size increased too. Formic acid[10] and hydrofluoric acid[13] were also used as modulators for the synthesis of micron-sized UiO-66 crystals with controlled morphology. Moreover, modulators promote the formation of defects in UiO-66 and these defects contribute to a higher surface area, which endows UiO-66 with improved gas uptake[14] and catalytic properties.[15]

To date, modulators have been frequently applied in the synthesis of UiO-66 and other Zr-based MOFs.[16] However, most of these modulators were used simply for reproducible preparation, improved crystallinity, enhanced porosity, and controlled size and morphology, but little attention was paid to employing the functionalities of the modulators themselves. In general, functionalities were introduced into MOFs either through the use of functional linkers or a post-modification strategy. Designing functional linkers allowed us to precisely introduce desired functionalities into MOFs but it's time-consuming and cost-intensive.[17,18] The post-modification approach allowed us to incorporate functionalities that were incompatible with *in situ* synthesis and to introduce different functionalities from the parent materials.[19] It also required that the parent MOF must be stable enough to endure the post-modification process and bear certain functionalities for post-modification. If the modulator bears

[a] *Shenzhen Key Laboratory of Laser Engineering, College of Optoelectronic Engineering, Shenzhen University, Shenzhen, 518060, P. R. China. E-mail: yjzeng@szu.edu.cn*
[b] *State Key Laboratory of Silicon Materials, School of Materials Science and Engineering, Zhejiang University, Hangzhou 310027, P.R. China. E-mail: pengxinsheng@zju.edu.cn*

† Electronic supplementary information (ESI) available. See DOI: 10.1039/c9ce00067d

certain functionalities, then, those aforementioned obstacles for introducing functionalities into MOFs can be avoided. Recently, Forgan *et. al*[20] and Shafir *et. al*[21] reported the synthesis of UiO-66 using amino acids as modulators independently. L-Proline was found to be not only an efficient modulator for the synthesis of single crystals, but also a functional-group which enhanced the CO_2 adsorption capability of UiO-66 through the interactions between CO_2 and the polar groups of L-proline.[21] The presence of L-proline in UiO-66 also made it an excellent chiral catalyst for the aldol addition reaction with better catalytic activity and diastereoselectivity than homogeneous L-proline.[22] Their pioneering work inspired us to explore other functional monocarboxylic acids which acted as modulators as well as functional groups to extend the application field of UiO-66.

Ferrocene is an organometallic compound composed of two cyclopentadienyl rings bound on opposite sides of a central iron atom.[23] Ferrocene and its derivatives have been well-known for their unique redox and electrochemical properties[24–27] and have been introduced into MOFs as redox-active centres through either post-synthetic modification[28–30] or physical encapsulation.[31,32] The embellishment of ferrocene expanded the application of MOFs in sensors,[31] selective gas separation,[32] redox catalysis,[29] *etc.* However, to the best of our knowledge, ferrocenecarboxylic acid (FcCOOH) has not been utilized as a modulator for the synthesis of UiO-66. Herein, we reported the synthesis of UiO-66 using FcCOOH as a modulator. The effects of the added amount of FcCOOH on the crystallinity, size and morphology, thermal stability and micro-structures of UiO-66 were studied. Ferrocene is a redox-active compound. Thus, the incorporation of FcCOOH endowed UiO-66 with redox properties, which were used to incorporate Pd nanoparticles into UiO-66-Fc by *in situ* reduction of the Pd^{2+} precursor. The resultant Pd@UiO-66 composite showed good catalytic activity in the Suzuki–Miyaura reaction and might be used for other organic syntheses.

2. Experimental

2.1. Reagents and chemicals

Zirconium tetrachloride ($ZrCl_4$, 98%), terephthalic acid (H_2BDC, 99%), 2-aminoterephthalic acid (98%) and iodobenzene (99%) were purchased from Aladdin. Phenylboronic acid (99%) and potassium tetrachloropalladate (K_2PdCl_4, 98%) were obtained from J&K Scientific Ltd. Ferrocenecarboxylic acid (FcCOOH, 99%) was supplied by Suzhou Time-Chem Technologies Co., Ltd. Anhydrous potassium carbonate (K_2CO_3, 99%), *n*-hexane (AR), isopropanol (AR) and *N*,*N*-dimethylformamide (DMF, AR) were purchased from Sinopharm Chemical Reagent Co., Ltd. All chemicals were used as received.

2.2. Synthesis of UiO-66-Fc

A series of UiO-66-Fc crystals were synthesized using different amounts of FcCOOH as a modulator. In a typical process, $ZrCl_4$ (116.2 mg, 0.5 mmol, 1 equiv.), H_2BDC (83.2 mg, 0.5 mmol, 1 equiv.) and different amounts of FcCOOH (0–20 equiv.) were dissolved in DMF (15 mL) under ultrasonic irradiation (25 °C, 10 min). The obtained solution was then transferred into a 25 mL Teflon-lined steel autoclave and placed in a preheated oven at 120 °C for 12 h. Powders were collected by centrifugation (3000 rpm, 30 min) and then washed with DMF and ethanol three times respectively. The obtained products were dried at 60 °C for 24 h. The detailed amounts of the reactants were provided in Table S1.† UiO-66 was synthesized using 10 equiv. of CH_3COOH as a modulator through the same synthetic procedure as that for UiO-66-Fc except FcCOOH was replaced with CH_3COOH. UiO-66-NH_2 was also synthesized using 10 equiv. of FcCOOH as a modulator through the same synthetic procedure as that for UiO-66-Fc except terephthalic acid was replaced with 2-aminoterephthalic acid (90.5 mg, 0.5 mmol).

2.3. Synthesis of Pd@UiO-66-Fc

Pd@UiO-66-Fc was synthesized by a one-step double solvent method.[33] Firstly, the UiO-66-Fc synthesized using 10 equiv. of FcCOOH as a modulator was activated at 160 °C under vacuum for 8 h. Then, the activated UiO-66-Fc (20 mg) was dispersed in *n*-hexane (20 mL), into which a K_2PdCl_4 (0.2 mL, 0.5 M) aqueous solution was added dropwise. The resultant dispersion was stirred vigorously (1500 rpm) at 25 °C for 3 h. Pd@UiO-66-Fc was obtained after centrifugation (3000 rpm, 30 min) and washed with deionized water three times to remove unreacted K_2PdCl_4. The final product was dried under vacuum at 35 °C for 48 h.

2.4. Suzuki–Miyaura reaction catalyzed using Pd@UiO-66-Fc

The Suzuki–Miyaura reaction was conducted according to a previous procedure[34] with minor modifications as follows. Pd@UiO-66 (7.8 mg), phenylboronic acid (91.7 mg, 0.75 mmol), iodobenzene (0.56 mL, 5.0 mmol) and K_2CO_3 (209 mg, 1.5 mmol) were dissolved into a mixture solvent of isopropanol (2.0 mL) and water (2.0 mL). The resulting mixture was stirred at 25 °C for 2 h. After completing the reaction, 10 mL of deionized water was added to dilute the solution. Then, Pd@UiO-66 was removed by centrifugation (3000 rpm, 30 min). The obtained solution was analysed by ^{1}H NMR to determine the conversion of phenylboronic acid.

2.5. Characterization methods

The powder X-ray diffraction data were collected on X-pert powder diffractometers (from 5–40°) using Cu Kα radiation sources (λ = 1.54178 Å). Scanning electron microscopy (SEM) images were taken on an Ultra 55 (V = 5 kV) instrument. Prior to measurements, all the samples were coated with gold for 2 min. High-resolution transmission electron microscopy (HR-TEM) images were obtained using a JEM 2100F instrument with an ultrathin carbon supporting film as the support. Transmission electron microscopy images were taken using a HT7700 TEM instrument. ^{1}H NMR spectra were recorded on

an Agilent DD2-600 NMR spectrometer. Thermal gravimetric analysis (TGA) was performed on a TA-Q500 (Mettler-Toledo) at a heating rate of 10 °C min^{-1} in a nitrogen atmosphere. N_2 sorption isotherms were recorded on a TriStar II instrument. Notably, all the samples were activated at 160 °C under vacuum for 8 hours prior to N_2 sorption isotherm measurements. Cyclic voltammetry (CV) was performed in a three-electrode electrochemical cell with a UiO-66-Fc modified working electrode, a Pt wire as the counter electrode and an Ag/AgCl reference electrode using a CHI 660D electrochemical workstation. The UiO-66-Fc modified working electrode was fabricated according to a previously reported procedure.[28] Firstly, about 3 mg of the sample was spread on a filter paper. Then, UiO-66-Fc was attached onto a clean glass carbon electrode (GCE) by gently rubbing the GCE over the sample. Fourier transform infrared spectroscopy (FT-IR) was performed on FT-IR TENSOR 27 equipment. ICP-AES was performed on an iCAP6300 after the samples were digested in *aqua regia* at 80 °C for 12 h. X-ray photoelectron spectroscopy (XPS) results were obtained using an ESCALAB_250Xi X-ray photoelectron spectrometer with Al Kα X-ray radiation as the excitation source.

3. Results and discussion

3.1. Modulated synthesis of UiO-66-Fc

To study the influence of FcCOOH, a series of UiO-66-Fc crystals (refer to UiO-66 synthesized using FcCOOH as a modulator) were synthesized with 0–10 equiv. (equiv. refers to the molar ratio between FcCOOH and $ZrCl_4$) of FcCOOH. The morphologies of the synthesized UiO-66-Fc were characterized using SEM. As shown in Fig. 1, UiO-66 synthesized without addition of FcCOOH tended to form inter-grown aggregates of small crystallites (about 400 nm). Increasing the added amount of FcCOOH (from 1–10 equiv.) resulted in UiO-66-Fc crystals with smaller size. In particular, when 6 or 10 equiv. of FcCOOH was added, UiO-66-Fc crystals with an average diameter of 50 nm were frequently observed. Notably, there was no obvious increase in the diameter of UiO-66-Fc when the reaction time was extended from 12 h to 24 h (Fig. 1f). For comparison, we also synthesized UiO-66 using 10 equiv. of CH_3COOH as a modulator. As shown in Fig. S1 and S2,† modulated with 10 equiv. of CH_3COOH, UiO-66 with a diameter of about 300 nm was obtained, which was much bigger than the UiO-66-Fc synthesized with 10 equiv. of FcCOOH. Generally, modulators (such as formic acid, acetic acid, benzoic acid and hydrofluoric acid) contribute to the formation of bigger crystals by suppressing nucleation. Considering that the molecule size of FcCOOH is much bigger than those of the aforementioned modulators, we speculate that steric effects may dominate the modulating effect. Once FcCOOH coordinated onto Zr nodes, it made the exchange between FcCOOH and H_2BDC difficult due to steric hindrance and thus resulted in the formation of smaller crystals. Further increasing the added amount of FcCOOH to 20 equiv., however, resulted in bulk FcCOOH crystals (Fig. S3†) which made the purification process much more difficult. Hence, we mainly focused on the synthesis of UiO-66-Fc with addition of 0–10 equiv. of FcCOOH as modulators.

Although the crystal size of the UiO-66-Fc crystals was quite small, they showed similar XRD patterns to UiO-66 (Fig. 2). Furthermore, the addition of FcCOOH improved the crystallinity of UiO-66 as the XRD patterns of UiO-66-Fc synthesized with addition of 1–10 equiv. of FcCOOH showed sharper and narrower diffraction peaks compared to that of the FcCOOH-free (0 equiv.) sample. Based on these data, FcCOOH was proved to be an effective modulator for the synthesis of high-quality UiO-66 crystals with diameters down to the nanometer scale. Besides, FcCOOH also improved the crystallinity of UiO-66-NH_2 (Fig. S4†). Without a modulator,

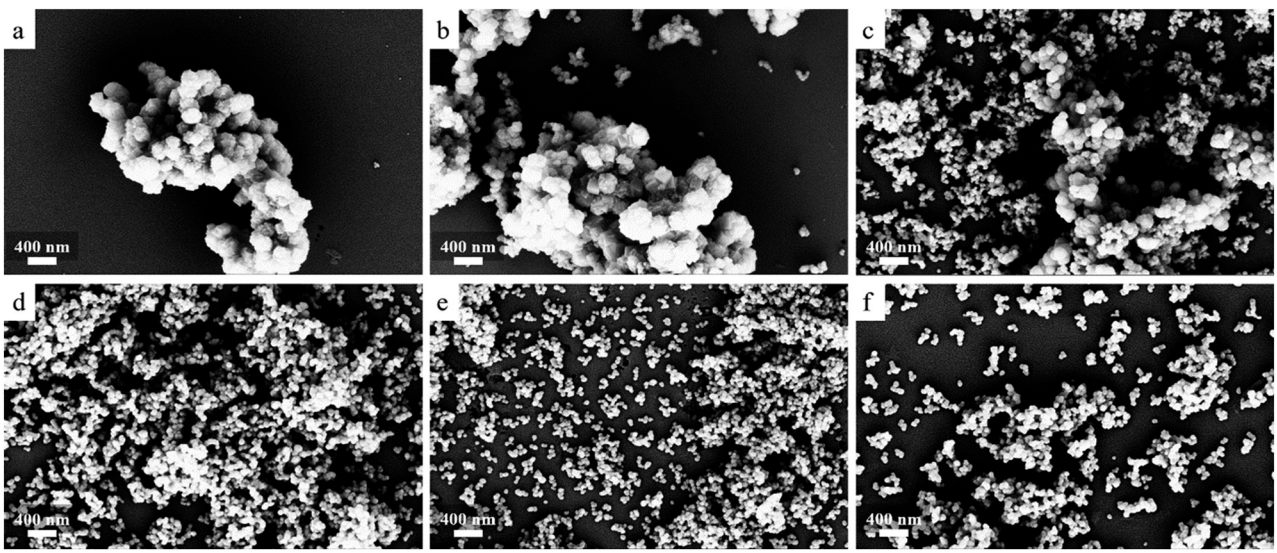

Fig. 1 SEM images of UiO-66-Fc synthesized with different equiv. of FcCOOH as modulators after a 12 h reaction: a) 0 equiv., b) 1 equiv., c) 2 equiv., d) 6 equiv., and e) 10 equiv. f) SEM image of UiO-66-Fc synthesized with 10 equiv. of FcCOOH as a modulator after a 24 h reaction.

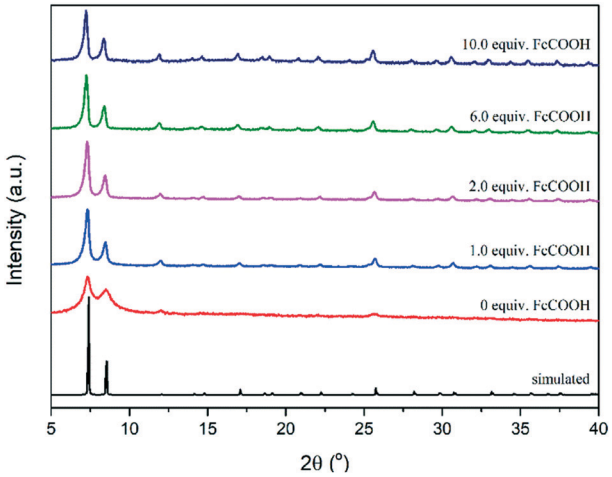

Fig. 2 XRD patterns of UiO-66-Fc synthesized with addition of different equiv. of FcCOOH.

we could only obtain UiO-66-NH_2 with poor crystallinity. Once 10 equiv. of FcCOOH was added during synthesis, UiO-66-NH_2 with higher crystallinity was obtained. We found that the XRD pattern of UiO-66-NH_2 was similar to that of UiO-66-Fc. This indicated that the synthesized UiO-66-NH_2 was isostructural to the UiO-66 framework topology. Thus, we deduced that FcCOOH was an efficient modulator that might be applied to synthesize other UiO-66-type MOFs with improved crystallinity.

The microstructures of UiO-66 were studied using N_2 isotherms. As shown in Fig. 3, all the samples showed a type I sorption isotherm. UiO-66-Fc synthesized with addition of FcCOOH showed better N_2 adsorption capacity. According to the obtained BET surface area data listed in Table S2,† the added amount of FcCOOH contributed to the larger BET surface area (1364 $m^2\ g^{-1}$) of UiO-66-Fc. Besides, both the micro-pore volumes (from 0.22 to 0.56 $cm^3\ g^{-1}$) and total pore volumes (from 0.30 to 1.21 $cm^3\ g^{-1}$) of UiO-66-Fc increased when the added equiv. of FcCOOH increased from 0 to 10 equiv. According to ref. 14 for a perfect UiO-66 crystal, the theoretical micro-pore volume and surface area are 0.426 $cm^3\ g^{-1}$ and 954 $m^2\ g^{-1}$, respectively. If 1 out of 12 linkers of the crystal is artificially removed for every metal centre in the unit cell (for a hypothetic model structure with ordered defects), the calculated values increase significantly to 0.502 $cm^3\ g^{-1}$ and 1433 $m^2\ g^{-1}$, respectively. As shown in Table S2,† both the micro-pore volume and BET surface area of non-modulated UiO-66 were lower than those of the perfect UiO-66 crystal. We ascribed it to its relatively low crystallinity (Fig. 2). When 6 equiv. of FcCOOH was added as a modulator, both the micro-pore volume (0.47 $cm^3\ g^{-1}$) and BET surface area (1106 $m^2\ g^{-1}$) were quite similar to the values of a perfect UiO-66 crystal. When 10 equiv. of FcCOOH was added as a modulator, the micro-pore volume (0.56 $cm^3\ g^{-1}$) and BET surface area (1364 $m^2\ g^{-1}$) were increased significantly and were close to the data of an ideal UiO-66 crystal with 1 missing defect in every metal centre in the unit cell. To be

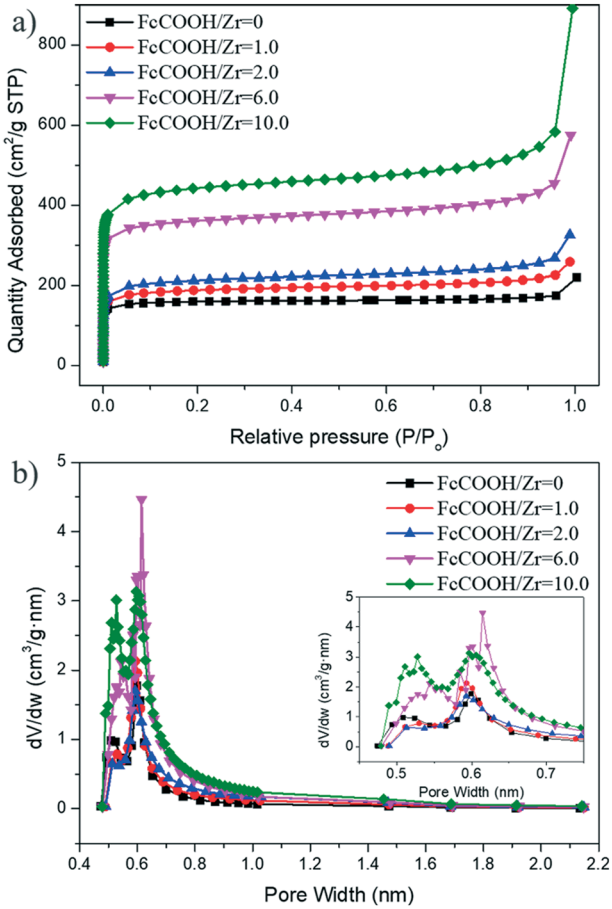

Fig. 3 N_2 adsorption isotherms (a) and pore size distribution (b) of UiO-66-Fc synthesized with addition of different equiv. of FcCOOH.

specific, addition of 10 equiv. of FcCOOH contributed to about 20% higher micro-pore volume and about 40% larger BET surface area than the calculated values for a perfect UiO-66 crystal. Although both the micro-pore volume and BET surface area were increased in UiO-66-Fc, the micro-pore diameters were almost unaffected (Fig. 3b). Thus, in light of these data, FcCOOH was demonstrated to be an effective modulator for the synthesis of UiO-66 with a larger pore volume and higher surface area.

The thermal properties of UiO-66-Fc were studied by TGA under a N_2 atmosphere. As shown in Fig. 4a, all the samples showed similar weight loss tendencies. The first stage, in the temperature range of 150–250 °C, was due to the removal of DMF. The second stage was ascribed to unresolvable weight losses of structural water (*i.e.* dehydroxylation) and coordinated FcCOOH. Notably, as the added equiv. of FcCOOH increased, more weight was lost in this stage indicating that more FcCOOH existed in UiO-66-Fc. An obvious weight loss was observed over a temperature range of 350–580 °C. This was due to the collapse of the MOF framework (decomposition of H_2BDC). It was observed that the addition of FcCOOH affected the starting and final decomposition temperatures of this stage. As evidenced by DTGA (Fig. S5†), both the starting and final decomposition temperatures of UiO-66 decreased

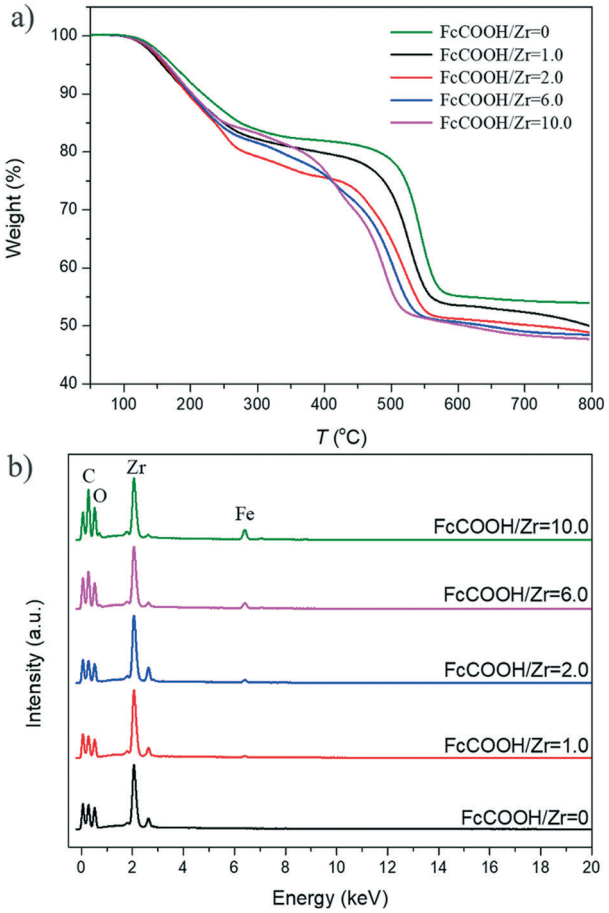

Fig. 4 TGA curves (a) and EDS patterns (b) of UiO-66-Fc synthesized with addition of different equiv. of FcCOOH.

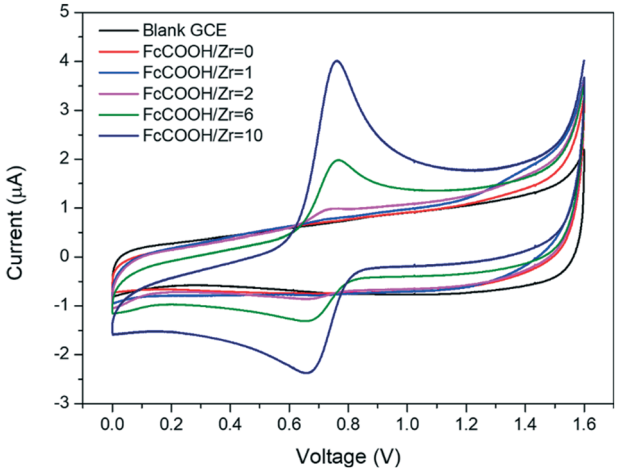

Fig. 5 Cyclic voltammetry curves of the blank glass carbon electrode and UiO-66-Fc modified glass carbon electrodes synthesized with addition of different equiv. of FcCOOH at a scanning rate of 0.1 V s^{-1}.

obviously as the added equivalent amount of FcCOOH increased from 0–10 equiv. Interestingly, addition of 10 equiv. of CH_3COOH during synthesis seemed to have no effect on the thermal stability of UiO-66, as the TGA curve (Fig. S6†) of UiO-66 synthesized with addition of 10 equiv. of CH_3COOH was very similar to that of UiO-66 synthesized without a modulator. We ascribed this to more defects found in UiO-66-Fc than in UiO-66 synthesized using CH_3COOH, and these defects contributed to the easier collapse of the MOF framework and thus compromised the thermal stability of UiO-66-Fc. According to the literature,[35] the linker deficiencies of UiO-66 can be quantified based on the TGA data. However, this method cannot be applied in our case because the existence of iron in FcCOOH makes the assumption that the TGA product observed at 550 °C is pure ZrO_2 used for quantitative analysis invalid.

Monocarboxylic acids used as modulators in the synthesis of UiO-66 have been proved to more than just provide an intermediate reactant and modulate the formation of MOF crystals. They also promoted the formation of defects by terminating the metal nodes.[13,14] Thus, we supposed that some FcCOOH may coordinate onto the nodes which contributed to the formation of defects in UiO-66-Fc. An increase in the BET surface area and micro-pore volume supported this assumption. Furthermore, the evidence of FcCOOH incorporation into UiO-66-Fc was provided by the EDS data. As shown in Fig. 4b, the peak intensity of iron at 6.3 keV increased as the added equiv. of FcCOOH increased. Considering the rough accuracy of EDS, it was not suitable to use these data for quantitative analysis. But the relative molar ratio of Fe/Zr indeed makes sense. As shown in Fig. S7,† the Fe/Zr molar ratio of UiO-66-Fc increased when more FcCOOH was added as a modulator. Subsequently, the exact amount of FcCOOH in UiO-66-Fc was determined by ICP-AES (Table S3†). The content of FcCOOH in UiO-66-Fc increased when the added amount of FcCOOH increased. To be specific, 27.7 wt% of FcCOOH existed in UiO-66-Fc when 10 equiv. of FcCOOH was added during synthesis. Besides, the calculated Fe/Zr molar ratio was consistent with the EDS results (Fig. S7†). These results indicated that FcCOOH was indeed incorporated into UiO-66-Fc.

However, it's still unknown whether FcCOOH was coordinated onto the nodes or just occluded in the pores of UiO-66-Fc as a free acid. We tried to distinguish the coordinated and uncoordinated FcCOOH in UiO-66-Fc through FT-IR (Fig. S8†). Compared with the modulator-free sample, there was a weak but recognizable peak at 1476 cm^{-1} assigned to the cyclopentadiene ($\nu_{-C=C-}$) of FcCOOH in the FT-IR spectra of UiO-66-Fc synthesized with 2–10 equiv. of FcCOOH. However, it's too weak to distinguish the coordination state of FcCOOH in UiO-66-Fc. According to the literature,[14,35] monoacid modulators (*e.g.* acetic acid, difluoroacetic acid, or trifluoroacetic acid) have been proved to coordinate onto some metal clusters to promote defects and porosity. Similarly, in our case, we thought that FcCOOH might also coordinate onto some metal nodes since more defects were observed when more FcCOOH was added during synthesis.

3.2. Redox properties of UiO-66-Fc

Ferrocene has been well-known for its unique redox properties, and has been found to have wide applications in

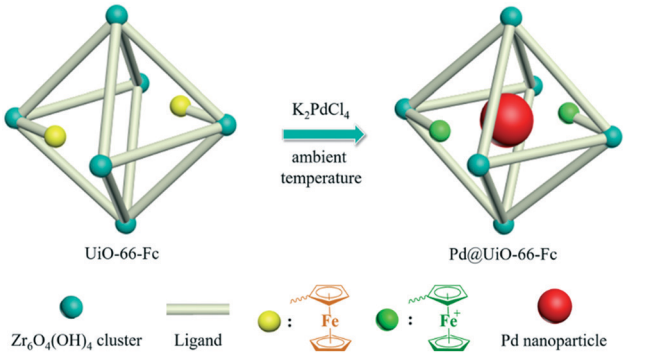

Scheme 1 Scheme of the incorporation of Pd nanoparticles into UiO-66-Fc through *in situ* reduction of Pd^{2+} into Pd nanoparticles by ferrocene carboxylate coordinated onto the $Zr_6O_4(OH)_4$ nodes.

stimuli-responsive materials.[36] Cyclic voltammetry (CV) is a convenient and efficient way to study the redox properties of ferrocene. Thus, the redox properties of UiO-66-Fc were investigated by CV in CH_2Cl_2 solution with 0.1 M *n*-Bu_4NBF_4 as the electrolyte. As shown in Fig. 5, at a scanning rate of 0.1 V s^{-1}, the blank GCE, UiO-66 and UiO-66-Fc synthesized with addition of 1 equiv. of FcCOOH showed no obvious redox peak in the range of 0–1.6 V. In contrast, redox waves ascribed to ferrocene/ferrocenium (Fc^+/Fc) were observed with a half wave potential ($E_{1/2}$) of about 0.71 V in the CV curves of UiO-66-Fc synthesized with addition of 2–10 equiv. of FcCOOH. What's more, it seems that an increase of FcCOOH/Zr had a negligible influence on $E_{1/2}$ (Table S4†). Notably, the redox potential of FcCOOH in 0.1 M *n*-Bu_4NBF_4/CH_2Cl_2 solution was 0.678 V, while the redox potential of UiO-66-Fc synthesized with addition of 10 equiv. of FcCOOH was 0.713 V, which shifted to a more positive potential compared with FcCOOH (Fig. S9†). According to ref. 37 this shift was attributed to the formation of coordination bonds between the carboxylate and the metal cation. Hence, we thought that this redox potential shift was evidence that FcCOOH coordinated onto the metal nodes.

The influence of the scanning rate (v, varied from 0.1–0.5 V s^{-1}) on the peak potential and peak current of Fc^+/Fc in UiO-66-Fc was studied (Fig. S10†) and was summarized in Table S4.† Since there were no obvious redox peaks for the blank GCE, UiO-66 and UiO-66-Fc synthesized with addition of 1 equiv. of FcCOOH, they were thus excluded in Table S4.† According to Table S4,† both the oxidation and reduction peak potential values (E_{pa} and E_{pc}) seemed to be independent of the scanning rate, which indicated a fast electron transfer that was limited by transport or finite diffusion.[28] Meanwhile, the peak currents (i_{pa} and i_{pc}) showed a linear dependence on the square roots of the scanning rate (Fig. S11†), indicative of electron transfer controlled by the diffusion of electrons in UiO-66-Fc.[37] Based on these results, we concluded that the incorporation of FcCOOH endowed UiO-66-Fc with excellent redox properties.

3.3. Preparation of Pd@UiO-66-Fc

We noted that the half wave potential of Fc^+/Fc in UiO-66-Fc was about +0.71 V, which was lower than that of Pd^{2+}/Pd (+0.91 V). Hence, the ferrocenyl group in UiO-66-Fc can be used to incorporate Pd nanoparticles into UiO-66-Fc through *in situ* reduction of the Pd^{2+} precursor (Scheme 1). As shown in Fig. 6a, Pd nanoparticles with diameters of 3–5 nm marked with red circles were frequently observed in Pd@UiO-66-Fc. The HAADF-STEM results and EDS line scan of Pd@UiO-66-Fc indicated that the bright nanoparticles in UiO-66-Fc (Fig. 6b and c) were Pd nanoparticles and their diameter was about 4 nm. Besides, both the EDS (Fig. S12†) and XPS results (Fig. S13†) of Pd@UiO-66-Fc indicated the presence of Pd elements in Pd@UiO-66-Fc. Furthermore, the amount of Pd in Pd@UiO-66-Fc was measured to be 4.27 wt% by ICP-AES. These results revealed that UiO-66-Fc was capable of reducing Pd^{2+} into Pd nanoparticles. Since the UiO-66 synthesized using CH_3COOH as a modulator showed no ability to reduce Pd^{2+} into Pd nanoparticles without addition of extra reductants, we thus deduced that it was the FcCOOH incorporated into UiO-66-Fc that functioned as the reducing agent which reduced Pd^{2+} into Pd nanoparticles. It was worth mentioning that the mild conditions (ambient temperature and without using an extra reductant) required in this procedure made UiO-66-Fc a promising support for incorporation of Pd nanoparticles without compromising the structure of the MOFs. As shown in Fig. S14,† the morphology of UiO-66-Fc

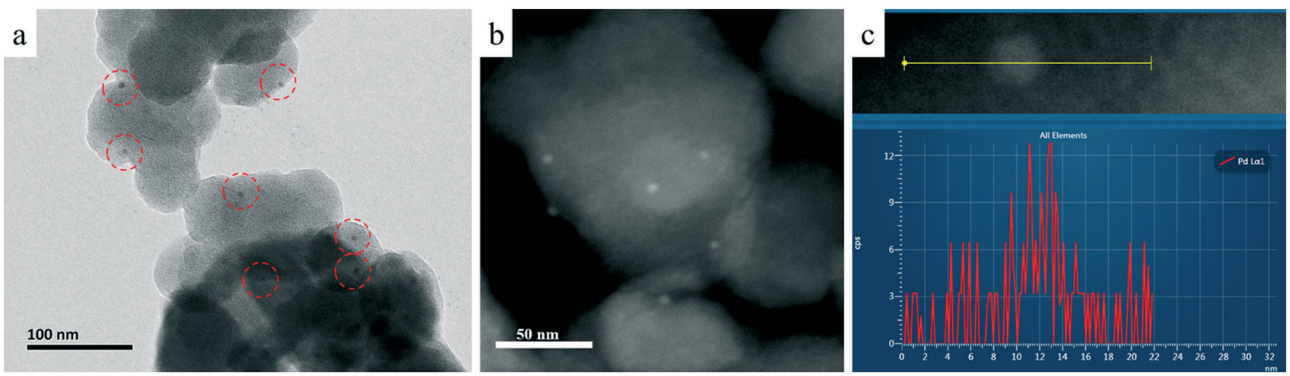

Fig. 6 TEM image (a), HAADF-STEM (b) and EDS line scan (c) of Pd@UiO-66-Fc (other elements were omitted for clarity).

before and after loading of Pd nanoparticles showed no obvious difference. Besides, the diffraction peaks of Pd@UiO-66-Fc were similar to those of UiO-66-Fc (Fig. S15†). These results indicated that the *in situ* reduction procedure had a negligible effect on the crystallinity of UiO-66-Fc. The absence of characteristic diffraction peaks of Pd nanoparticles might be due to their small size and relatively low loading amount.

Palladium has been widely used as a catalyst for various kinds of organic syntheses.[38–40] Therefore, we envisioned that the obtained Pd@UiO-66-Fc might find potential applications in heterogeneous catalysis. As a proof of concept, Pd@UiO-66-Fc was utilized as a heterogeneous catalyst for the Suzuki–Miyaura reaction and the reaction was traced *via* ^{1}H NMR. As shown in Fig. S16,† the characteristic chemical shift of phenylboronic acid at 7.9 ppm almost disappeared after reaction for 2 h. Based on the integration of the characteristic chemical shift of phenylboronic acid at 7.9 ppm and the characteristic chemical shift of biphenyl at 7.65 ppm (Fig. S17†), the overall conversion of phenylboronic acid was calculated to be 95%. These results indicated that Pd@UiO-66-Fc was indeed an efficient heterogeneous catalyst for the Suzuki–Miyaura reaction and might find applications in other organic syntheses.

4. Conclusions

In summary, we have demonstrated for the first time that FcCOOH is an efficient modulator for the synthesis of UiO-66 with a higher degree of crystallinity, smaller crystal size, larger pore volume and higher BET surface area. This method can also be extended to synthesize other UiO-66-type MOFs (such as UiO-66-NH_2). FcCOOH not only serves as a modulator but also endows UiO-66 with redox properties, which can be used for incorporation of Pd nanoparticles through *in situ* reduction. This reduction process occurs at room temperature without addition of extra reducing agents, and thus prevents MOFs from being damaged. The nano-meter size, high BET surface area and presence of Pd nanoparticles make Pd@UiO-66 a promising heterogeneous catalyst for the Suzuki–Miyaura reaction.

Conflicts of interest

There are no conflicts to declare.

Acknowledgements

This work was supported by the National Basic Research Program of China 973 Program (2015CB655302), the National Key Research and Development Program (2016YFA0200204), the Key Program of National Natural Science and Foundation (NSFC 51632008), the National Natural Science Foundations of China (NSFC 21671171, 21875212), the Major R & D plan of Zhejiang Natural Science Foundation (LD18E020001) and the Shenzhen Science and Technology Project under Grant No. KQJSCX20170727101208249 and JCYJ20170412105400428.

Notes and references

1 D. Farrusseng, S. Aguado and C. Pinel, *Angew. Chem., Int. Ed.*, 2009, **48**, 7502–7513.
2 Y. Mao, J. Li, W. Cao, Y. Ying, P. Hu, Y. Liu, L. Sun, H. Wang, C. Jin and X. Peng, *Nat. Commun.*, 2014, **5**, 6532.
3 A. Morozan and F. Jaouen, *Energy Environ. Sci.*, 2012, **5**, 9269–9290.
4 K. Sumida, D. L. Rogow, J. A. Mason, T. M. McDonald, E. D. Bloch, Z. R. Herm, T.-H. Bae and J. R. Long, *Chem. Rev.*, 2012, **112**, 724–781.
5 Y. Mao, D. Chen, P. Hu, Y. Guo, Y. Ying, W. Ying and X. Peng, *Chem. – Eur. J.*, 2015, **21**, 15127–15132.
6 J.-R. Li, J. Sculley and H.-C. Zhou, *Chem. Rev.*, 2012, **112**, 869–932.
7 Y. Mao, W. Cao, J. Li, Y. Liu, Y. Ying, L. Sun and X. Peng, *J. Mater. Chem. A*, 2013, **1**, 11711–11716.
8 J. H. Cavka, S. Jakobsen, U. Olsbye, N. Guillou, C. Lamberti, S. Bordiga and K. P. Lillerud, *J. Am. Chem. Soc.*, 2008, **130**, 13850–13851.
9 G. Wissmann, A. Schaate, S. Lilienthal, I. Bremer, A. M. Schneider and P. Behrens, *Microporous Mesoporous Mater.*, 2012, **152**, 64–70.
10 J. Ren, H. W. Langmi, B. C. North, M. Mathe and D. Bessarabov, *Int. J. Hydrogen Energy*, 2014, **39**, 890–895.
11 A. Schaate, P. Roy, A. Godt, J. Lippke, F. Waltz, M. Wiebcke and P. Behrens, *Chem. – Eur. J.*, 2011, **17**, 6643–6651.
12 M. J. Katz, Z. J. Brown, Y. J. Colon, P. W. Siu, K. A. Scheidt, R. Q. Snurr, J. T. Hupp and O. K. Farha, *Chem. Commun.*, 2013, **49**, 9449–9451.
13 Y. Han, M. Liu, K. Li, Y. Zuo, Y. Wei, S. Xu, G. Zhang, C. Song, Z. Zhang and X. Guo, *CrystEngComm*, 2015, **17**, 6434–6440.
14 H. Wu, Y. S. Chua, V. Krungleviciute, M. Tyagi, P. Chen, T. Yildirim and W. Zhou, *J. Am. Chem. Soc.*, 2013, **135**, 10525–10532.
15 F. Vermoortele, B. Bueken, G. Le Bars, B. Van de Voorde, M. Vandichel, K. Houthoofd, A. Vimont, M. Daturi, M. Waroquier, V. Van Speybroeck, C. Kirschhock and D. E. De Vos, *J. Am. Chem. Soc.*, 2013, **135**, 11465–11468.
16 Z. Hu, Y. Peng, Z. Kang, Y. Qian and D. Zhao, *Inorg. Chem.*, 2015, **54**, 4862–4868.
17 A. Schaate, P. Roy, T. Preusse, S. J. Lohmeier, A. Godt and P. Behrens, *Chem. – Eur. J.*, 2011, **17**, 9320–9325.
18 F. Drache, V. Bon, I. Senkovska, C. Marschelke, A. Synytska and S. Kaskel, *Inorg. Chem.*, 2016, **55**, 7206–7213.
19 V. Valtchev, G. Majano, S. Mintova and J. Perez-Ramirez, *Chem. Soc. Rev.*, 2013, **42**, 263–290.
20 R. J. Marshall, C. L. Hobday, C. F. Murphie, S. L. Griffin, C. A. Morrison, S. A. Moggach and R. S. Forgan, *J. Mater. Chem. A*, 2016, **4**, 6955–6963.
21 O. V. Gutov, S. Molina, E. C. Escudero-Adan and A. Shafir, *Chem. – Eur. J.*, 2016, **22**, 13582–13587.
22 X. Feng, H. S. Jena, K. Leus, G. Wang, J. Ouwehand and P. Van der Voort, *J. Catal.*, 2018, **365**, 36–42.
23 F. S. Arimoto and A. C. Haven, *J. Am. Chem. Soc.*, 1955, **77**, 6295–6297.

24 Z. Deng, H. Yu, L. Wang and X. Zhai, *J. Organomet. Chem.*, 2015, **791**, 274–278.
25 Z. Deng, H. Yu, L. Wang, X. Zhai, Y. Chen and R. Sun, *J. Organomet. Chem.*, 2015, **799-800**, 273–280.
26 Z. Deng, L. Wang, H. Yu, X. Zhai, Y. Chen, A. Zain ul and N. M. Abbasi, *RSC Adv.*, 2016, **6**, 29663–29668.
27 Z. Deng, H. Yu, L. Wang, X. Zhai, Y. Chen and S. Z. Vatsadze, *J. Organomet. Chem.*, 2016, **821**, 48–53.
28 J. E. Halls, A. Hernan-Gomez, A. D. Burrows and F. Marken, *Dalton Trans.*, 2012, **41**, 1475–1480.
29 I. Hod, W. Bury, D. M. Gardner, P. Deria, V. Roznyatovskiy, M. R. Wasielewski, O. K. Farha and J. T. Hupp, *J. Phys. Chem. Lett.*, 2015, **6**, 586–591.
30 I. Hod, O. K. Farha and J. T. Hupp, *Chem. Commun.*, 2016, **52**, 1705–1708.
31 Z. Chang, N. Gao, Y. Li and X. He, *Anal. Methods*, 2012, **4**, 4037–4041.
32 W. Zhang, D. Banerjee, J. Liu, H. T. Schaef, J. V. Crum, C. A. Fernandez, R. K. Kukkadapu, Z. Nie, S. K. Nune, R. K. Motkuri, K. W. Chapman, M. H. Engelhard, J. C. Hayes, K. L. Silvers, R. Krishna, B. P. McGrail, J. Liu and P. K. Thallapally, *Adv. Mater.*, 2016, **28**, 3572–3577.
33 A. Aijaz, A. Karkamkar, Y. J. Choi, N. Tsumori, E. Roennebro, T. Autrey, H. Shioyama and Q. Xu, *J. Am. Chem. Soc.*, 2012, **134**, 13926–13929.
34 A. W. Augustyniak, W. Zawartka, J. A. R. Navarro and A. M. Trzeciak, *Dalton Trans.*, 2016, **45**, 13525–13531.
35 G. C. Shearer, S. Chavan, S. Bordiga, S. Svelle, U. Olsbye and K. P. Lillerud, *Chem. Mater.*, 2016, **28**, 3749–3761.
36 C. G. Hardy, J. Zhang, Y. Yan, L. Ren and C. Tang, *Prog. Polym. Sci.*, 2014, **39**, 1742–1796.
37 K. Hirai, H. Uehara, S. Kitagawa and S. Furukawa, *Dalton Trans.*, 2012, **41**, 3924–3927.
38 H. Li, C. C. C. Johansson Seechurn and T. J. Colacot, *ACS Catal.*, 2012, **2**, 1147–1164.
39 D. Sun and Z. Li, *J. Phys. Chem. C*, 2016, **120**, 19744–19750.
40 G. Huang, Q. Yang, Q. Xu, S.-H. Yu and H.-L. Jiang, *Angew. Chem., Int. Ed.*, 2016, **55**, 7379–7383.